Available online at www.sciencedirect.com
ScienceDirect
Geochimica et Cosmochimica Acta 71 (2007) 5876–5887
Geochimica et Cosmochimica Acta
www.elsevier.com/locate/gca

Molecular models of a hydrated calcite mineral surface

Thomas D. Perry IV [a,*], Randall T. Cygan [b], Ralph Mitchell [a]

[a] Harvard School of Engineering and Applied Sciences, Cambridge, MA 02138, USA
[b] Sandia National Laboratories, Albuquerque, NM 87185-0754, USA

Received 25 September 2006; accepted in revised form 30 August 2007; available online 9 October 2007

Abstract

Hydrated mineral surfaces play an important role in many processes in biological, geological, and industrial applications. An energy force field was developed for molecular mechanics and molecular dynamics simulations of hydrated carbonate minerals and was applied to investigate the behavior of water on the $(10\bar{1}4)$ calcite surface. The force field is a significant development for large-scale molecular simulations of these systems, and provides good agreement with experimental and previous modeling results. Simulations indicate that water molecules are significantly ordered near the calcite surface. The predominant surface configuration (75–80%) results from coordination of a water molecule with a single calcium cation–carbonate anion pair, while the less common situation involves water coordination with two ion pairs. Surface restructuring and variation in coordination in the water layers results in distinct distances for water oxygens above the calcite surface—a two-component first monolayer (2.3 and 3.0 Å) and a secondary monolayer (5.0 Å). The different coordinations also alter lateral displacement, hydrogen bonding, and surface-normal orientation of the water molecules. The ordering of water molecules and the formation of a unique hydrogen bonding network at the calcite surface influence the physical properties of the interfacial water. Surface exchange of water molecules is observed by molecular dynamics simulation to occur at a rate of one exchange per 10 ps. Diffusion coefficients derived from mean square displacement analysis of atomic trajectories indicate a dependence of water transport based on the distance of the water molecules from the calcite surface.

1. INTRODUCTION

Calcite is one of the most abundant minerals in the environment and is fundamentally important in a variety of fields. The $(10\bar{1}4)$ family of crystal faces is the most stable (Hwang et al., 2001) and by far the dominant observed morphology of calcite *in situ* (Didymus et al., 1993). In the environment, calcite dissolution and precipitation are important regulators of global carbon cycling (Schlesinger, 1997), the chemistry of marine systems (Pilson, 1998), the local pH and alkalinity of terrestrial environments (Stumm and Morgan, 1996), aquifer heterogeneity and hydrologic complexity (Stumm, 1992), and adsorption processes of heavy metals and contaminant transport (Reeder et al., 2001). In industrial systems, heat-transfer efficiency is reduced by the growth of calcareous mineral scales (Stahl et al., 2000), and in biological systems calcite is an important ingredient in biomineralization (Teng et al., 1998). Most, if not all, of the important reactions for these systems occurs in aqueous environments, and a fundamental understanding of the chemistry of the calcite surface interacting with water molecules and aqueous solutes is essential.

Many research groups have helped develop our understanding of calcite surface behavior using a variety of experimental and theoretical techniques (Fenter et al., 2000; Wright et al., 2001; Kerisit et al., 2003; Rohl et al., 2003; Geissbühler et al., 2004; Kerisit et al., 2005). Fortunately, recent advances in computing and processor speeds have allowed molecular simulation to become a powerful tool for predictive modeling of interactions in these complex systems. However, the validity of the simulations is rooted in developing the appropriate parameters to accurately describe a given system, especially for a system too large to

* Corresponding author. Current address: Harvard Business School, Boston, MA 02163, USA. Fax: +1 617 496 1471.
E-mail address: tperry@seas.harvard.edu (T.D. Perry).

0016-7037/$ - see front matter © 2007 Elsevier Ltd. All rights reserved.
doi:10.1016/j.gca.2007.08.030

be accurately described by state-of-the-art electronic structure methods. Additionally complicated are heterogeneous systems, especially those involving interfaces, where molecular dynamics simulations require the transfer of energy and momentum across an interface. For example, cleavage of a calcite crystal will lead to a carbonate surface that atomically rearranges in response to water exposure that will, in turn, form hydration layers in response to the structure of the substrate and associated electrostatic potential.

Predictive molecular simulation requires development of empirical energy force fields that can accurately simulate inter- and intra-molecular interactions in complex, heterogeneous systems with different molecular types (Kollman, 1996). Development of an energy force field to accurately describe the structure and energy of calcite and calcite–water systems has received significant attention over the last 10 years (Pavese et al., 1992; Titiloye et al., 1993; de Leeuw and Parker, 1997; Titiloye et al., 1998; Fisler et al., 2000; Hwang et al., 2001; Wright et al., 2001; Cygan et al., 2002; Duckworth et al., 2003; Kerisit et al., 2003; de Leeuw and Cooper, 2004; Duffy and Harding, 2004; Kerisit and Parker, 2004a,b). However, most of the initial efforts to simulate calcite surfaces and calcite–water interfaces relied on interaction parameters derived from bulk calcite systems (e.g., Pavese et al., 1992 and Fisler et al., 2000). Simulations involving shell models, especially those that allow for electronic polarization of carbonate oxygen (e.g., Wright et al., 2001, Kerisit et al., 2003, Kerisit and Parker, 2004a) provide an improved approach for the combined atomistic and electronic relaxation of carbonate surfaces and a more accurate response of water molecules in large electrostatic potentials. However, these computational methods are somewhat difficult to implement (e.g., Lamoureux and Roux, 2003), especially for large-scale simulations (many tens and hundreds of thousands of atoms for perhaps a million time steps), and often require specialized software. With the inclusion of additional interaction terms, the shell-based water models typically improve the descriptions of the structure of water but often at the expense of accuracy in predicting thermodynamic values (Chen et al., 2000; Chialvo et al., 2000; Rick and Stuart, 2002). In order to provide an alternative approach for the computational chemist, we have developed a simple yet accurate force field for calcite–water systems that uses the rigid ion approximation and Lennard–Jones (12–6) potentials for nonbonded interactions that can be easily incorporated in most academic and commercial software codes.

In the current study, we develop a molecular mechanics force field for the classical simulation (molecular dynamics and Monte Carlo methods) of calcite and calcite-aqueous interfaces, and which includes flexible water molecules to represent the explicit hydration of the calcite surface. The parameters for water molecules are derived from a modified simple point charge (SPC) water model (Berendsen et al., 1981), which has previously been shown to accurately predict water dynamic and structural properties (van der Spoel et al., 1998). The SPC model was modified to include terms for molecular flexibility (Teleman et al., 1987) that can potentially be used to asses molecular vibrations using velocity autocorrelation methods (e.g., Corongiu and Clementi, 1993). Parameters for the calcite were complied from previous theoretical studies of various carbonate minerals (Fisler et al., 2000; Duckworth et al., 2003) and combined with those for flexible SPC water model. The force field herein is an improvement on alternate models because it incorporates atomic and molecular flexibility that more reliably reproduces the transfer of momentum during dynamic simulations, which can have important effects on physical properties such as atomic relaxation and diffusion processes near an interface. A complete description of the force field is presented, as well as results from molecular dynamics simulation for the hydration effects on calcite structure, arrangement of water molecules on the common $(10\bar{1}4)$ calcite surface, and the effect of water configuration on physical properties. The theoretical results are also compared to recent experimental studies.

2. METHODS

2.1. Force field theory and development

An energy-based empirical force field was developed for modeling carbonate minerals with explicit water hydration. Parameters for calcite were developed (Fisler et al., 2000; Duckworth et al., 2003), and a single point charge (SPC) water model (Berendsen et al., 1981) was used to parameterize the water interactions (Cygan et al., 2004). The flexible SPC model relies on implicit hydrogen bonding, which reduces the number of force field parameters while maintaining modeling accuracy. The simple water parameters used in this study are an attractive alternative to the shell model (Kerisit and Parker, 2004b) because they are computationally faster and more adaptable to similar modeling efforts while maintaining accurate structure and thermodynamics. The current force field describes the potential energy of a chemical system through summation of individual interatomic energies and the geometry of the molecular configurations as (Cygan, 2001):

$$E_{\text{total}} = E_{\text{Coul}} + E_{\text{VDW}} + E_{\text{bondstretch}} + E_{\text{anglebend}} + E_{\text{inversions}}, \quad (1)$$

where E_{Coul} and E_{VDW} are the non-bonded energy terms, and $E_{\text{bondstretch}}$, $E_{\text{anglebend}}$, and $E_{\text{inversions}}$ are the bonded energy terms, as will be discussed in detail following. The parameters for atoms (Table 1), non-bonded terms (Table 2), and bonded terms (Table 3) are summarized.

The Coulombic energy (E_{Coul}) is inversely proportional to the distance of separation (r) of the species (i, j) by:

Table 1
Atom descriptions and designations

Element	Description	Symbol	Charge (e)
H	Water hydrogen	h^*	0.4100
O	Water oxygen	o^*	−0.8200
O	Carbonate oxygen	o	−1.1145
C	Carbonate carbon	c	1.3435
Ca	Calcium	Ca	2.0000

Table 2
Non-bonded parameters for the force field

Interacting atoms			
Species *i*	Species j	R_o (Å)	D_o (kcal/mol)
o^*	o^*	3.5532	1.5540E−01
o	o^*	4.4266	6.9687E−05
o	*o*	5.9000	4.5000E−08
Ca	o^*	5.6000	3.4000E−04
Ca	*o*	4.9460	1.4555E−03
h	o^*	3.1516	7.6845E−02
h	*o*	4.0250	3.4460E−05
h^*	*o*	4.0250	3.4460E−05
ho	*o*	4.0250	3.4460E−05
h	*Ca*	3.6710	1.6051
c	o^*	3.8066	1.5165E−01

$$E_{\text{Coul}} = \frac{e^2}{4\pi\varepsilon_o}\sum_{i\neq j}\frac{q_i q_j}{r_{ij}} \tag{2}$$

where q are the partial charges (Table 1), e is the charge of an electron, and ε_O is the dielectric permittivity of vacuum. The equation represents a double summation over the interaction of atoms i and j, avoiding the evaluation of any repeat atom pairings ($i \neq j$).

The van der Waals energy (E_{VDW}) is represented by the Lennard–Jones (12–6) function using the convention of potential energy well depth D_0 at an equilibrium distance R_0. It contains short-range repulsions associated with the increase in energy as two atoms approach each other and the attractive dispersion energy:

$$E_{\text{VDW}} = \sum_{i\neq j} D_{o,ij}\left[\left(\frac{R_{o,ij}}{r_{ij}}\right)^{12} - 2\left(\frac{R_{o,ij}}{r_{ij}}\right)^{6}\right] \tag{3}$$

The empirical Lennard–Jones terms for atom pairs within the mineral surface (calcite calcium and carbonate oxygen, *Ca–o*; carbonate oxygen and carbonate oxygen, *o–o*) and for interfacial interactions such as calcite calcium and water oxygen (Ca–o^*) are derived from observed structural and physical property data, and were adapted to the force field by combination rules and conversions of Buckingham potentials taken from Fisler et al. (2000) and Duckworth et al. (2003) (Table 2). Comparison of modeling simulations with experimental work for the bulk and surface carbonate structures are detailed in these previous computational studies. Simulation results for the new force field were compared to the original set of simulations to confirm the accuracy of the new set of potentials. The calcium–water potential is consistent with other SPC-based water models used to describe the behavior of the solvated calcium ion (e.g., Åqvist, 1990, Koneshan et al., 1998). Note that atom type nomenclature is presented in the accompanying tables to distinguish among the various chemistries for any particular element (water oxygen versus carbonate oxygen; o^* versus *o*). Interaction parameters for other atom pairs were derived using standard combination rules for arithmetic distance (R_0) and geometric energy (D_0) parameters following (Halgren, 1992) (Table 2).

The bonded energy terms include bond stretch ($E_{\text{bondstretch}}$), angle bend ($E_{\text{anglebend}}$), and inversions ($E_{\text{inversions}}$). The bond stretch energy of the hydroxyl (o^*–h^*) in SPC water is described by a harmonic relationship:

$$E^{o^*-h^*}_{\text{bondstretch},ij} = \frac{1}{2}k_1(r_{ij} - r_o)^2 \tag{4}$$

where k_1 is a force constant and r_O represents the equilibrium bond length (Table 3). Alternately, a Morse potential is utilized to calculate the energy for carbonate bonds (*c–o*) via:

$$E^{c-o}_{\text{bondstretch},ij} = D_e(e^{-\alpha(r-r_o)} - 1)^2 \tag{5}$$

where D_e is the bond dissociation energy, α is a constant for the given bond dependent on the vibrational force constant, and r_O is the equilibrium bond distance (Table 3). The carbonate (*o–c–o*) and water (h^*–o^*–h^*) angle bend energy is described using a harmonic potential as:

$$E_{\text{anglebend},ijk} = \frac{1}{2}k_2(\theta_{ijk} - \theta_o)^2 \tag{6}$$

where k_2 is an empirical force constant and θ_o is the equilibrium bond angle (Table 3). The bond inversion energy of the carbonate anion results from out-of-plane distortion of the dihedral angle (φ) as calculated by a four-body (*c–o–o–o*) potential in:

Table 3
Bonded parameters for the force field

Species *i*	Species *j*	Potential	k_1 (kcal/mol Å^2)	r_o (Å)	
Bond stretch					
o^*	h^*	Harmonic	1108.2697	1	
Species *i*	Species *j*	Potential	D_e (kcal/mol)	α (Å^{-1})	r_o (Å)
c	*o*	Morse	1467.7156	1.294	115.3045
Species *i*	Species *j*	Species *k*	k_2 (kcal/mol rad^2)	θ_o (°)	
Angle bend					
h^*	o^*	h^*	91.5392	109.47	
o	*c*	*o*	49.4981	120	
Species *i*	Species *j*	Species *k*	Species *l*	k_i (kcal/mol)	
Inversions					
c	*o*	*o*	*o*	122.8	

$$E_{\text{inversion},ijkl} = \frac{1}{2}k_i(1+\cos\varphi)^2 \quad (7)$$

where k_i is a force constant (Table 3). The dihedral angle decreases and the inversion energy increases as the oxygen atom is deflected out of plane. The present force field includes a stronger inversion parameter (Rohl et al., 2003) than used in previous carbonate models, which was implemented in the static molecular simulations of Duckworth et al. (2003).

2.2. Modeling simulations and analysis

The dimensions of the simulation cell with periodic boundary conditions were $24.0 \times 29.7 \times 56.8$ Å and consisted of a 10 Å-thick vacuum region above a 34 Å-thick solution (water-filled) region above a 22 Å-thick substrate originally created from the $(10\bar{1}4)$ cleavage of calcite based on the experimental crystal structure (Effenberger et al., 1981). The $(10\bar{1}4)$ calcite surface is charge neutral, which assures that there is no significant polarization associated with any of the interfaces (calcite–water, water–vacuum, and calcite–vacuum) created by the slab model (Duckworth et al., 2003). At circumneutral conditions, the calcite surface is approximately neutral with charge separation (van Cappellen et al., 1993; Pokrovsky et al., 1999, 2000; Fenter et al., 2000; Pokrovsky and Schott, 2002; Duckworth et al., 2003; Salinas-Nolasco et al., 2004). Assuming equilibrium conditions for the calcite, protonated surface and solvated metal and bicarbonate species were omitted from the simulation cell. Dissociation constants and relative concentrations of charged species, their equilibrium contributions would be negligible compared to the net-neutral calcite surface for the circumneutral pH conditions; only Ca^{2+} and CO_3^{2-} surface species and their water associated complexes are examined. Fig. 1 provides a graphic representation of the periodic cell used in the molecular dynamics simulations.

Molecular simulations were performed using spline cutoffs of 8.0 Å and 8.5 Å for the short-range van der Waals interactions and long-range Ewald sums for Coulombic interactions (Tosi, 1964). All molecular dynamics simulations were performed as NVT canonical ensembles where volume and temperature conditions were maintained statistically constant (Allen and Tildesley, 1987). The vacuum gap created above the solution (liquid–vapor interface) assures equilibration to the appropriate density of the aqueous phase where the water (or aqueous solution) can freely expand or compress. A Nosé–Hoover thermostat (Hoover, 1985) maintained at 300 K was used to control temperature during the simulations with a relaxation time of 0.1 ps. The Verlet velocity algorithm was used to obtain accurate integration of the dynamics equations and statistical ensembles (Verlet, 1967). Simulations were allowed to equilibrate using a 1-fs time step for an initial 100 ps period followed by a 1-ns production period for obtaining equilibrium statistics on energy and structure. The results of the molecular dynamics simulations are derived from analysis of the complete 1 ns atomic trajectories.

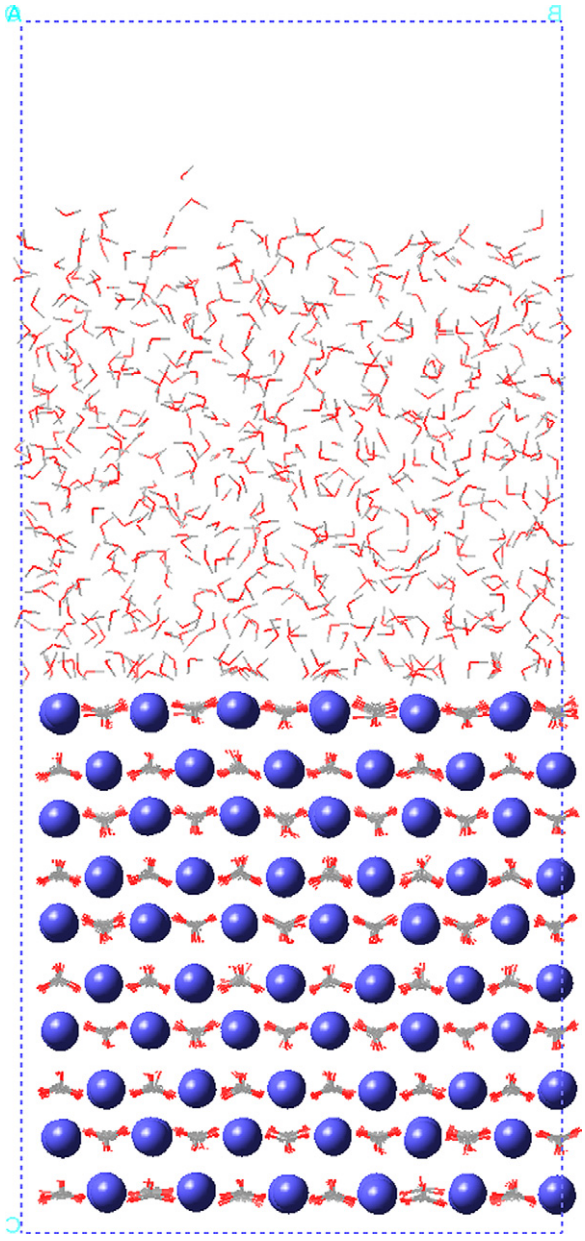

Fig. 1. Snapshot of simulation cell from molecular dynamics showing the bulk crystal terminating at the $(10\bar{1}4)$ face, a multilayered water-solvated region, and a region of vacuum. Atoms are colored coded as follows: calcium (blue), oxygen (red), carbon (dark grey), hydrogen (light grey).

3. RESULTS AND DISCUSSION

Molecular dynamics simulations of explicit water molecules on the $(10\bar{1}4)$ surface of calcite were conducted. The periodic slab-based simulation cell includes approximately ten layers of water molecules capped by a vacuum space to allow expansion and contraction of the water region. The large-scale simulations take advantage of a relatively simple fully-flexible force field to accurately reproduce the structure of the calcite–water interface. The results of the simulations are organized as follows: the effects of

hydration on calcite structure, the structure and configuration of water layers on the mineral surface, and the effects of surface water organization on physical properties of water, such as the rates of molecular water exchange on the calcite surface and water diffusion.

3.1. Hydration effects on calcite structure

The surface structure of the mineral as influenced by water is important for understanding calcite dissolution and reactivity. We observed that water molecules strongly interact with the $(10\bar{1}4)$ calcite surface and attenuate the degree of relaxation normally associated with the calcite surface when exposed in vacuum (de Leeuw and Parker, 1998; Fisler et al., 2000; Duckworth et al., 2003). The molecular simulations suggest an equilibrium system of alternating layers of calcium with variable ion spacing and carbonate group inversions. Additionally, the simulations provide insights regarding the ranges of atomic motion not necessarily obtained through traditional static energy optimizations.

Water molecules and their hydrogen-bonding network affected the displacement of calcium ions in the calcite structure. In an idealized crystal structure without molecular rearrangement or surface relaxation, the $(10\bar{1}4)$ planes with calcium ions are separated from each other by 3.03 Å (in the z-axis direction for the simulation cell). The mean outward displacement of the calcium ions of the surface layer in our simulation are 0.12 Å (relative to an unrelaxed structure) with a variation of 0.11 Å. While the variation is larger than the experimental observations of Geissbühler et al. (2004) (0.017 ± 0.004 Å), the molecular dynamics simulation provides reasonable agreement for the mean displacement. The atomic relaxations in the uppermost layer require that subsequent layers restructure in an alternating fashion to accommodate strain on the crystal lattice (Wright et al., 2001). In the calcite layers closest to the water molecules, calcium ions are displaced out of the bulk position toward the aqueous phase. The attraction of the positively charged cations into the water region is primarily the result of the strong electrostatic interaction with the negatively-charged SPC oxygen and its attempt to complete the calcium coordination sphere (Wright et al., 2001). Lateral displacements of the calcium ions are also observed and typically vary by about 0.3 Å from the equilibrium position (see Geissbühler et al., 2004). A similar surface relaxation for calcium ions was observed at the vacuum exposed surface of the slab model.

The configuration of water molecules on the surface also influences the inversion angles of the carbonate anions in the calcite substrate. These inversions increase bond strain and energy but serve to stabilize van der Waals and Coulombic forces caused by atom displacements throughout the system (Wright et al., 2001). Inversion is associated with a four-body potential and the deflection of carbonate oxygen atoms out of the plane of the carbonate anion; it is an independent of relaxation and tilting of the entire carbonate group into the bulk crystal structure. An idealized, planar carbonate group will have a null inversion angle ($\varphi = 0°$). Displacement of the carbonate oxygen atoms out-of-plane into solution resulted in a positive inversion angle, while a negative angle indicated bending towards the vacuum region. In our simulations, the greatest inversion angles were observed on the calcite interior ($\bar{\varphi} = 2.0 \pm 1.7°$). However, the hydrogen bonding among surface water molecules appeared to stabilize the most exterior carbonate groups with $\bar{\varphi} = 1.4 \pm 1.6°$. The surface carbonate monolayers are less inverted than in the bulk, presumably because of the stabilization of the carbonate groups by hydrogen bonding with the surface water molecules.

The movement of calcium ions and changes in carbonate inversions are coincidental. For example, when calcium ions are displaced into the aqueous region, there is a correlated inversion of carbonate bonds towards the water. The concurrent alternating pattern for calcium ion displacement and carbonate inversion was apparent. These synchronized movements are likely the result of long-range Coulombic interactions of the calcium ions and the partial negative charges on the carbonate oxygen atoms.

3.2. Arrangement of water on the $(10\bar{1}4)$ calcite surface

As much as water affects the calcite surface structure, the potential energy topology—controlled by Coulombic and van der Waals forces at the calcite surface—affects surface water organization. Radial distribution functions (RDF or $g(r)$) performed on manually selected water layers from our simulations demonstrate the variation in interatomic distances for several atom pairs (Fig. 2). The distance between oxygen atoms of the first monolayer of water molecules (o^*–o^*) is tightly organized with a dominant peak for an adjacent water molecule near 2.9 Å, similar to the simulation results of Kerisit et al. (2003). The second monolayer and bulk water molecules exhibit a similar peak with successively decreasing g(r) near 2.8 Å. The slight difference in RDF between the first and outer layers is associated with the distances between the surface water molecules

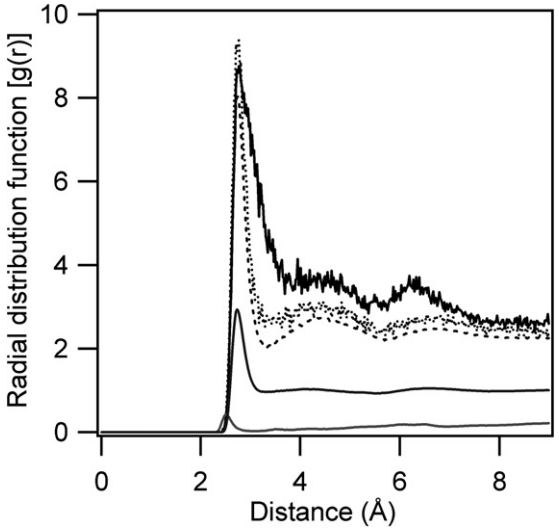

Fig. 2. Interatomic radial distribution functions for: first monolayer o^*–o^* (solid black), second monolayer o^*–o^* (small dash black), bulk o^*–o^* (large dash black), o^*–o^* bulk water (dark grey), and Ca–o^* (light grey).

(hydrogen bond distances) being extended due to strong interactions with the highly charged calcium (and carbonate) ions in the mineral surface.

The RDF of the oxygen atoms of the water molecules in the presence of the $(10\bar{1}4)$ calcite surface is similar to that obtained for oxygen derived from a bulk water simulation (Fig. 2). A molecular dynamics simulation representing bulk water was performed for 512 water molecules as an NVT canonical ensemble, similar to simulations completed for the calcite–water interface. Excluding the slight perturbation in the first water monolayer, the RDF peak for nearest-neighbor oxygen are similar in both simulations, indicating that the calcite surface did not significantly affect water molecule spacing in layers above the first water monolayer. However, the 0.1-Å shift in the RDF of the first monolayer indicates that water molecules are slightly laterally spread across the surface by interaction with the calcite calcium cations and carbonate anions thereby increasing the o^*–o^* $g(r)$.

In our data, the RDF of the first monolayer of water exhibits a second major peak at 6.3 Å (Fig. 2). We attribute the dominant RDF peaks to two types of surface coordinated water molecules. The RDF peak at 2.9 Å is the dominant single coordination water molecules; the RDF peak at 4.5 Å is due to tetrahedral ordering of water molecules due to hydrogen bonding with other water molecules; and the peak at 6.3 Å is associated with the separation of water molecules induced by double-coordinated water molecules (viz. Fig. 4). In their simulations with lower partial charges assigned to the atoms of the carbonate anion, Kerisit et al. (2003) observed a dominant peak at 4.725 Å, which they attributed to modification of the surface water structure by interaction with calcite calcium cations. The discrepancies between the modeling measurements in this study and in Kerisit et al. (2003) on the lateral displacement of water molecules in the first monolayer, and the resulting changes in properties, will continue to be a challenge to reconcile with the experimental results of Geissbühler et al. (2004).

Density profiles derived from the simulations of the atom types near the $(10\bar{1}4)$ calcite surface further demonstrate the ordering of water molecules in two surface coordination modes. Water molecules are controlled, in part, by the position of calcium ions and orientation of carbonate anions in the immediate calcite surface. The complete hydration of these charged surface features and their complex topology are important determinants of water molecule ordering and physical properties as has been observed experimentally (Geissbühler et al., 2004). For a given calcium carbonate molecular pair on the $(10\bar{1}4)$ calcite surface, two oxygen atoms are oriented diagonally out of the mineral surface plane, and one is positioned in the opposite direction. The orientation alternates by layer (detailed side view of Fig. 1; see Fig. 4 of Duckworth et al., 2003). The carbonate carbon atoms and calcium ions reside between these oxygen atoms (Fig. 3a). In our simulations, relaxation of the exterior-most carbonate oxygen atoms into the mineral bulk is observed (Fig. 3a) (Duckworth et al., 2003; Fenter et al., 2000; Fenter and Sturchio, 1999; Geissbühler et al., 2004; Kerisit et al., 2003; Rohl et al., 2003; Wright et al., 2001), reducing the effective surface corrugation. The density profiles of atoms near the calcite surface reveal insights about their coordination and orientation at the surface. There is a dominant water oxygen (o^*) density peak O_{W1} with secondary peaks O_{W2} and O_{W3} (Fig. 3A). Following previous convention (Geissbühler et al., 2004; Kerisit and Parker, 2004a), the O_{W1} and O_{W2} water layers are both components of the first water layer, while O_{W3} is the second water layer. The z-axis position of $O_{W1}(z_1)$, $O_{W2}(z_2)$, and $O_{W3}(z_3)$ above the calcite $(10\bar{1}4)$ surface, as defined by the plane of mean calcium ion position, is similar to several previous experimental and theoretical studies (Table 4). Lateral (xy) displacement and orientation of the water molecules in our studies are also similar to previous experimental and simulation studies (Geissbühler et al., 2004; Kerisit and Parker, 2004a, respectively).

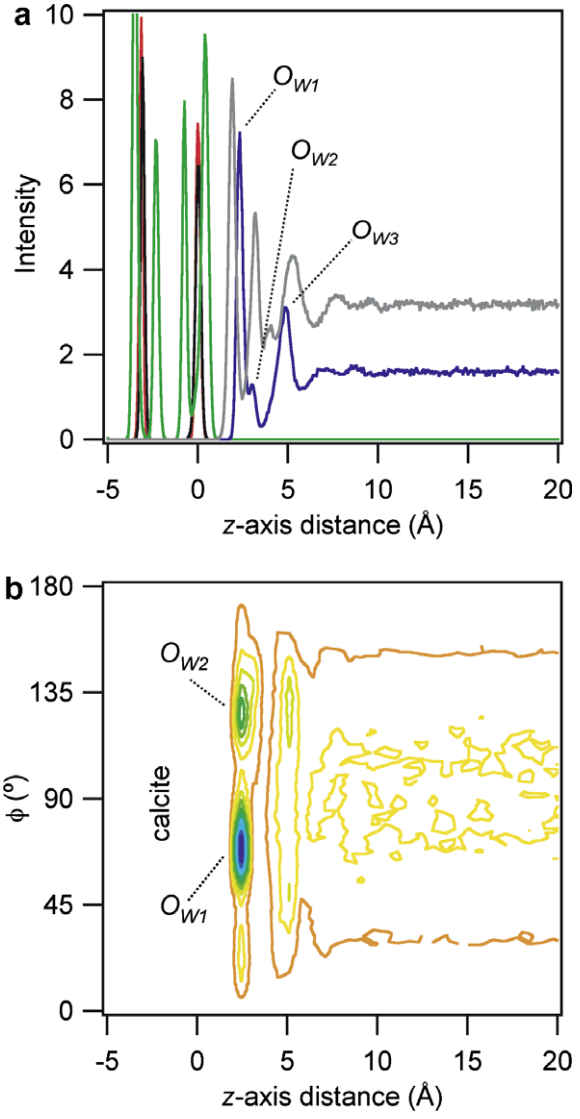

Fig. 3. (a) Atomic density profiles near the $(10\bar{1}4)$ calcite surface for water atoms, o^* (blue), h^* (grey) and calcite atoms, Ca (red), c (black), and o (green). (b) Contour plot of water molecule dipole orientation normal to the calcite surface (arbitrary units).

Table 4
Comparison of experimental and theoretical parameters of water monolayers on the $(10\bar{1}4)$ calcite surface

Technique	z_1 (Å)	z_2 (Å)	z_3 (Å)	Ref.
X-ray scattering	2.3 ± 0.1	3.45 ± 0.2	5.25	Geissbühler et al. (2004)
X-ray scattering	2.5 ± 0.12	—	—	Fenter et al. (2000)
Modeling	2.2	3.2	5.0	Kerisit and Parker (2004a)
Modeling	2.38[a]			Kerisit et al. (2003)
	2.37[b]			
	2.45[c]			
Modeling	2.55	—	—	Wright et al. (2001)
Modeling	2.4	—	—	de Leeuw and Cooper (2004)
Modeling	2.3	3.0	5.0	This study

[a] Atomistic model.
[b] Electronic structure calculation.
[c] Molecular dynamics simulation.

We attribute the O_{W1} peak to single coordination of water molecules with the calcite surface, where a water molecule interacted and formed hydrogen bonds with a single calcium ion and carbonate group (Fig. 4a). The O_{W2} is attributed to double coordination with the surface, where a water molecule interacts with two sets of surface carbonate groups (Fig. 4a). These arrangements are consistent with the position of the hydrogen atoms of both the O_{W1} and O_{W2}, with the hydrogen atoms pointing toward carbonate oxygen atoms in the calcite surface (Hwang et al., 2001; Wang et al., 2005). The O_{W1} and O_{W2} carbonate-associated hydrogen atoms are combined in the h^* peak at 1.9 Å, which results in the relatively high intensity of this peak (Fig. 3a). The lone hydrogen held away from the surface in O_{W1} results in the h^* peak at 3.2 Å, which is appropriate for the covalent water bond held perpendicular to the calcite surface. The O_{W3} peak is associated with the second water layer. The dual surface water arrangements are also supported by the relative peak intensities of O_{W2} to O_{W1} (0.23) compared to observed frequency of double—versus single—coordination (0.20) based on the counts of the surface water position in the simulation cell at multiple time steps.

The water molecules are distinctly arranged in two surface arrangements as characterized by their dipole orientations normal to the surface. Water molecules were bisected by their dipole in the charge-positive to charge-negative direction following standard convention. Dipole orientation of the water molecule was classified according to the disposition of the bisector angle relative to the vector normal to the calcite surface (Wang et al., 2005). The water dipole angle with $0° < \phi < 90°$ is characterized by a water oxygen oriented towards the surface with the hydrogens directed away, while at $90° < \phi < 180°$ the opposite occurs (viz. Fig. 4b). In the first water layer two major orientations normal to the surface are apparent (Fig. 3b). Most water molecules are oriented near the surface with single coordination (O_{W1}) have an average dipole angle orientation of $\overline{\phi_{O_{W1}}} = 68°$. The double coordinated (O_{W2}) water molecules have an average orientation of $\overline{\phi_{O_{W2}}} = 143°$. There is also some organization of the second water layer with similar orientations as well as a consistent range of orientations that avoid the 0° and 180° extremes. These data further support defining the bi-distribution of water molecule orientations near the calcite surface.

Hydrogen bonding is involved in the ordering of water molecules near the calcite surface and in the bulk aqueous phase. The type and total number of hydrogen bonds experienced by water molecules and variation of the average fraction of water molecules with different numbers of hydrogen bonds as a function of distance from the calcite surface can be compared as has been done previously for muscovite-water system (Wang et al., 2005). There are approximately two hydrogen bonds per water molecule in the first water layer (2 Å) near the calcite surface (Fig. 5a). This number increases moving further into the bulk solution with a slight dip at the transition into the second water layer (3.5 Å) resulting from the coincidental declining interaction of carbonate interactions and increasing bulk water interactions. The bulk water equilibrates at an average of 3.5 hydrogen bonds per water molecule at >5 Å with carbonate interactions no longer evident. The number of hydrogen bonds associated with each water molecule also is variable depending on the proximity to the calcite surface. There is a single dominant peak of water molecules with two hydrogen bonds at 1.6 Å (Fig. 5b), which is the result of the presence of only single-coordinated water molecules closely bound to the calcite surface at this distance (viz. Fig. 4a). However, the first water layer also includes O_{W2} water molecules having on average three and four hydrogen bonds at an average distance of 3.1 Å. Water molecules at $1.7 > \text{Å} > 2.5$, experience a mixture of one, two, and three hydrogen bonds. Hence, beyond this first water layer the transition into the second water layer results in a decline in total hydrogen bonding. Above 4 Å, the bulk water structure is approached with increasing importance of four hydrogen bonded water molecules and equilibrium bulk water is achieved at >5 Å with three and four hydrogen bonded water as the major species. Near the water–vapor interface (at approximately 24 Å), the number of hydrogen bonds experienced by each water molecule steadily declines; this change in bonding is the result of the vapor state of the molecules and not due to long-range surface properties. These details of the hydrogen bonding are consistent with our previous description of water orientations near the calcite surface, and confirm that the water behavior in the bulk phase is similar to previous simulation work (van der Spoel et al., 1998; Wang et al., 2005).

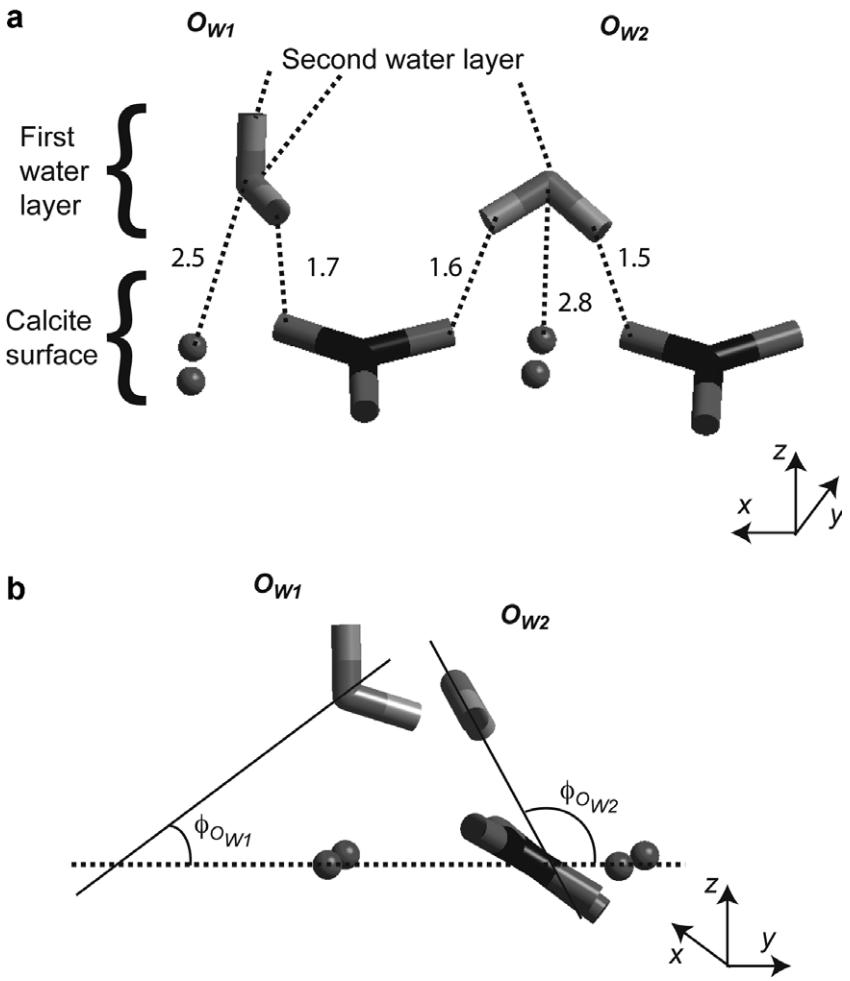

Fig. 4. Schematic of the different surface water coordination arrangements associated with O_{W1} and O_{W2} from two view points. In the first (a), dashed lines represent non-bonded *Ca–o** and *o–h** interactions and show the distances between interacting atoms in Angstroms. The second view point (b) shows a 90° rotated view with representations of the water dipole normal to the calcite surface (Water orientation pictures are descriptive of surface orientation but do not represent the average value; images were created from a single snapshot of the dynamics simulation.). Atoms are color coded similar to Fig. 3a.

Molecular dynamic simulations performed by Kerisit and Parker (2004a) determined that the different modes of adsorption in the first monolayer (O_{W1} vs. O_{W2}) occur in a 1:1 ratio as determined by their similar adsorption free energies. Other modeling efforts for hydrated calcite systems found that surface water molecules lay flat on the surface in alternating orientations but these simulations were performed using only a water monolayer (de Leeuw and Parker, 1997; Kerisit et al., 2003). The robustness of our force field parameter set may allow for additional insights into the dynamic properties of the water molecules as determined by their surface coordination and hydrogen bonding with the upper water layers, and may be more reliable because of the effect on important surface-mediated properties, namely surface exchange of water and the near-surface diffusion of water.

Molecular simulations provide additional insights that may not be accessible by experimental techniques, specifically in cases where small numbers and relative mobility of individual atoms are masked by other processes. Geissbühler et al. (2004) stated: "the lower [*z*-axis] height for O_{W1} suggests a chemical interaction with the calcite surface, while the larger height for O_{W2} suggests...a weaker, non-specific interaction with the calcite surface." Our simulations indicate that the double coordination of O_{W2} is a stronger, or, at least more, stable interaction. Fig. 6 shows contours of the relative atomic densities of atoms at the calcite–water interface. Single-coordinated water molecules are the dominant surface species. However, double-coordinated water molecules can also be observed, such as those highlighted in Fig. 6. These water molecules are less mobile on the calcite surface, as evidenced by the more dense contours indicating that the water molecules are more fixed than O_{W1} water molecules, in disagreement with the suggestion of Geissbühler et al. (2004). The authors of this previous study rationalized that the closer physical association of the O_{W1} oxygen atoms with the calcite calcium ions resulted in stronger surface interactions. We suggest that, although the O_{W2} oxygen atoms are further from the surface, the double coordination and additive effect of both

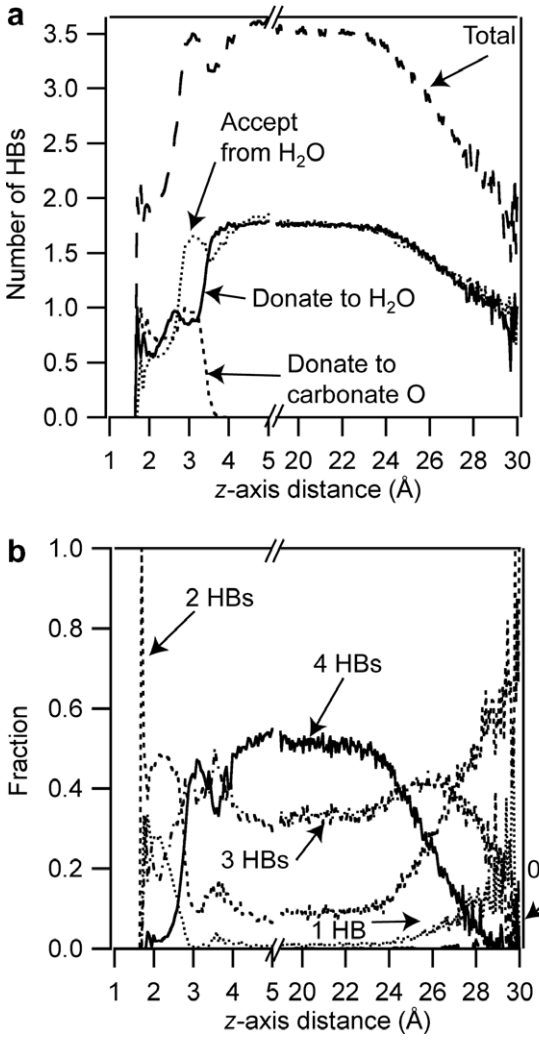

Fig. 5. (a) Type and total number of hydrogen bonds experienced by water molecules (a) and variation of the average fraction of water molecules with different numbers of hydrogen bonds (b) in relation to distance from the calcite surface.

water hydrogen atoms held close to the surface (viz. Figs. 3a, 4a, and 5b) result in a greater net surface stability and less molecular translation of the waters. Molecular modeling provides additional information about the atomistic detail of atomic interactions that can have dramatic import. For example, understanding the arrangement of water molecules at the surface assists in the determination of the adsorption of aqueous ions. Also, the major effect of double coordination on surface ordering of water molecules may play a role in the observed large entropy change of water molecules near the $(10\bar{1}4)$ calcite surface (Geissbühler et al., 2004; Kerisit and Parker, 2004a).

3.3. Effect of water arrangement on physical properties

The disposition of water molecules at the calcite surface affects important physical properties including exchange and transport processes. The strong association of the water molecules resulting from the surface charge distribution controls the exchange rate of water molecules. It appears that under our simulation conditions, double coordinated waters (O_{W2}) do not readily exchange as those that are single coordinated (O_{W1}), as indicated by the relative density of contour lines in Fig. 6.

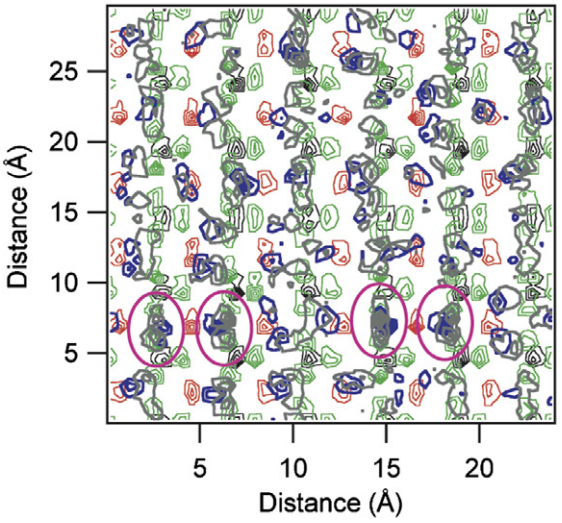

Fig. 6. Atomic density contours of water on the $(10\bar{1}4)$ calcite surface at 200 ps. Double coordinated (O_{W2}) molecules are circled in the plot for the 200-ps data set. Atoms are color coded similar to Fig. 3.

Considering all water molecules in the first monolayer, we observe a consistent water molecule exchange rate (Fig. 7d). Water molecules were only considered exchanged when they moved away from the surface and another water molecule, either from the bulk or the surface, replaced their position on the surface. All exchanged water molecules remained in the bulk and did not reform a surface association during this simulation. In the initial 200 ps of the equilibrated molecular dynamics simulation, water molecules that were originally associated with the calcite surface were able to move approximately half way (15 Å) across the periodic simulation cell in the z-axis (Fig. 7a–c). Conversely, water molecules originally close to the water–vacuum interface, were capable of traversing the entire water region (30 Å) in the same time period (Fig. 7e and f). The strong calcite–water interactions influences the water exchange rate, which limits movement of the water molecules into the bulk solution, and, therefore, how far they can diffuse in a given time period. Additionally, only single coordinated (O_{W1}) water molecules successfully exchanged at the surface, while O_{W2} molecules maintained surface associations and position during the first 200 ps of the simulation. However, O_{W2} molecules do exchange with sufficient simulation time and further affected the properties of water at the surface. Presumably, modification of the simulation conditions, such as increased temperature, would allow augmented exchange of the double coordinated water molecules.

The strength of the calcite–water interactions also influences the diffusion rate of the water molecules in these systems. We observe an average diffusion rate of 2.1×10^{-9} $m^2\ s^{-1}$ for water molecules near the calcite–water interface. Diffusion rates are derived from the analysis of mean square

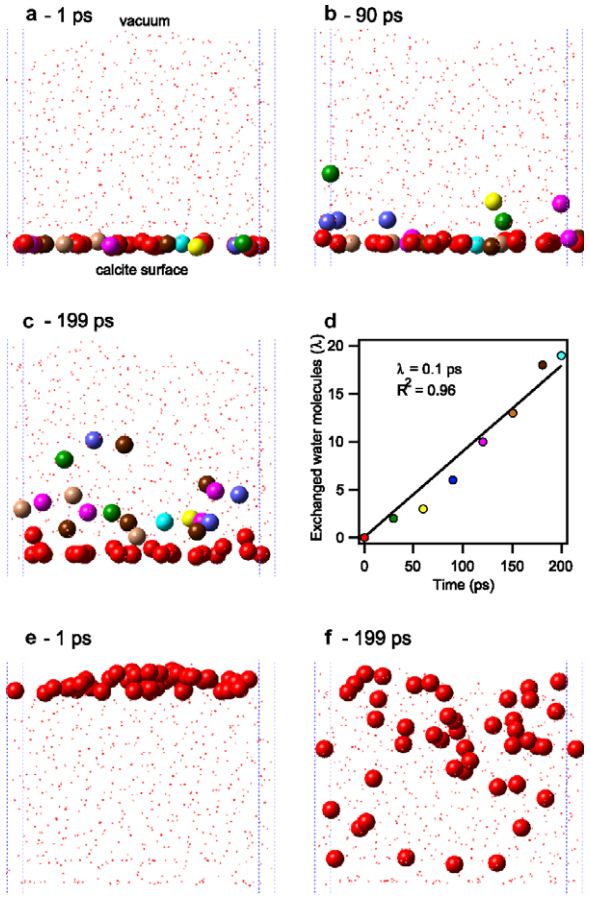

Fig. 7. (a–c) Time series simulation screen captures of exchanging water molecules on the $(10\bar{1}4)$ calcite surface obtained from the molecular dynamics trajectory. Only O_{W1} water molecules exchanged during this simulation period. Water oxygen molecules are visible for clarity and have been color-coded according to when they are exchanged at the surface (viz. d). The vacuum and calcite labels in (a) are consistent for all screen captures. (d) Summary of the number of exchanged water molecules (λ) over time with a line fit to the resulting data. (e, f) In comparison, water molecules from the same simulation at the vacuum interface (all red) have significantly more mobility in the medium over the same time period. These data were collected for the first 200 ps of the simulation.

displacements of water oxygen atoms from the atomic trajectories; bin volumes of water molecules were examined every 3 Å from the calcite surface. The first monolayer of water molecules exhibit a slower self-diffusion rate than those of the second monolayer, and those in bulk water (Kerisit and Parker, 2004a) due to the interactions with the calcite surface. The third monolayer of water (the third monolayer of water is further from the surface than O_{W3}) approximates bulk-like water behavior with no apparent surface water structuring (viz. Figs. 3 and 4) and provides a diffusion rate that is in agreement with rates modeled in the absence of a calcite surface. Additionally, the simulated bulk water diffusion rate D in the presence ($D = 2.7 \times 10^{-9}$ m^2 s^{-1} at 10.5 Å from the surface) and absence of calcite ($D = 2.7 \times 10^{-9}$ m^2 s^{-1}) are in general agreement with experimental results of Krynicki et al. (1978) ($D = 2.3 \times 10^{-9}$ m^2 s^{-1}). Water dissociation and surface speciation may affect the diffusion rates of surface-associated water molecules but we assume these factors to be of secondary importance, at least for the circumneutral pH conditions of the simulation.

4. CONCLUSIONS

A relatively simple energy force field for molecular dynamics simulation of calcite with explicit hydration was developed. The bond stretch and angle bend terms added to the conventional rigid SPC water model are important for accurately modeling the physical properties of water, especially for describing water behavior at an interface such as calcite. The combination of the flexible SPC water model with a rigid ion calcite force field accurately reproduces more sophisticated simulation approaches while providing reasonable agreement with experimental observations. The fully flexible water model is competitive with other popular water models, namely rigid SPC, extended simple point charge (SPC/E), and the three point (TIP3P) and four point (TIP4P) transferable intermolecular potentials, but these other models are less practical and not easily incorporated with carbonate parameters (van der Spoel et al., 1998). The calcite–water force field can be modified to include interaction terms for other important carbonate phases (Duckworth et al., 2003), including those containing the major cations Cd, Mn, Fe, Zn, Co, Ni, and Mg.

The force field was successfully applied to a one-nanosecond dynamics simulation of a hydrated calcite $(10\bar{1}4)$ surface. The surface structure of calcium cations and carbonate anions of the calcite are both modified in the presence of water by alternating displacement and inversion, respectively. The water molecules are highly ordered on the calcite surface and two unique coordination configurations are observed, refining previously unexplained experimental results. Self-diffusion rates were calculated and are in good agreement with experimental observations. The developed force field will be important in the modeling of chemical behavior at carbonate mineral surfaces. Further additions and refinements of the energy force field will allow for inclusion of organic components such as acids, ligands, and other calcite-affecting species, and for modeling of the interactions of these chemicals in a dynamic aqueous system.

ACKNOWLEDGMENTS

This work was supported in part by a Campus Executive Fellowship to Perry through the Laboratory Directed Research and Development Program at Sandia National Laboratories. Cygan also acknowledges the support provided by the Chemical Sciences, Geosciences, and Biosciences Division of the Office of Basic Energy Sciences in the U.S. Department of Energy. Sandia is a multiprogram laboratory operated by Sandia Corporation, a Lockheed Martin company, for the U.S. Department of Energy under Contract DE−AC04-94AL85000.

REFERENCES

Allen M. P., and Tildesley D. J. (1987) *Computer Simulation of Liquids*. Oxford University Press, Oxford.

Åqvist J. (1990) Ion–water interaction potentials derived from free energy perturbation simulations. *J. Phys. Chem.* **94**, 8021–8024.

Berendsen H. J. C., Postma J. P. M., van Gunsteren W. F., and Hermans J. (1981) Interaction models for water in relations to protein hydration. In *Intermolecular Forces* (ed. B. Pullman). D. Reidel, Dordretcht, p. 331.

Chen B., Xing J. H., and Siepmann J. I. (2000) Development of polarizable water force fields for phase equilibrium calculations. *J. Phys. Chem. B* **104**(10), 2391–2401.

Chialvo A. A., Yezdimer E., Driesner T., Cummings P. T., and Simonson J. M. (2000) The structure of water from 25 °C to 457 °C: Comparison between neutron scattering and molecular simulation. *Chem. Phys.* **258**(2–3), 109–120.

Corongiu G., and Clementi E. (1993) Molecular dynamics simulations with a flexible and polarizable potential: density of states for liquid water at different temperatures. *J. Chem. Phys.* **98**(6), 4984–4990.

Cygan R. T. (2001) Molecular modeling in mineralogy and geochemistry. In *Molecular Modeling Theory: Applications in the Geosciences*, vol. 42 (eds. R. T. Cygan and J. D. Kubicki). Mineralogical Society of America, Chantilly VA, pp. 1–35.

Cygan R. T., Liang J.-J., and Kalinichev A. G. (2004) Molecular modeling of hydroxide, oxyhydride, and clay phases and the development of a general force field. *J. Phys. Chem. B* **108**, 1255–1266.

Cygan R. T., Wright K., Fisler D. K., Gale J. D., and Slater B. (2002) Atomistic models of carbonate minerals: Bulk and surface structures, defects, and diffusion. *Mol. Simulat.* **28**, 475–495.

de Leeuw N. H., and Cooper T. G. (2004) A computer modeling study of the inhibiting effect of organic adsorbates on calcite crystal growth. *Cryst. Growth Des.* **4**(1), 123–133.

de Leeuw N. H., and Parker S. C. (1997) Atomistic simulation of the effect of molecular adsorption of water on the surface structure and energies of calcite surfaces. *J. Chem. Soc. Faraday Trans.* **93**(3), 467–475.

de Leeuw N. H., and Parker S. C. (1998) Surface structure and morphology of calcium carbonate polymorphs calcite, aragonite, and vaterite: an atomistic approach. *J. Phys. Chem. B* **102**, 2914–2922.

Didymus J. M., Oliver P., Mann S., DeVries A. L., Hauschka P. V., and Westbroek P. (1993) Influence of low-molecular-weight and macromolecular organic additives on the morphology of calcium carbonate. *J. Chem. Soc. Faraday Trans.* **89**(15), 2891–2900.

Duckworth O. W., Cygan R. T., and Martin S. T. (2003) Linear free energy relationships between dissolution rates and molecular modeling energies of rhombohedral carbonates. *Langmuir* **20**, 2938–2946.

Duffy D. M., and Harding J. H. (2004) Simulation of organic monolayers as templates for the nucleation of calcite crystals. *Langmuir* **20**(18), 7630–7636.

Effenberger H., Mereiter K., and Zemann J. (1981) Crystal structure refinements of mangesite, calcite, rhodochrosite, siderite, smithsonite, and dolomite, with discussion of some aspects of the stereochemistry of calcite type carbonates. *Z. Kristallogr.* **156**, 233–243.

Fenter P., Geissbühler P., DiMasi E., Srajer G., Sorensen L. B., and Sturchio N. C. (2000) Surface speciation of calcite observed in situ by high-resolution X-ray reflectivity. *Geochim. Cosmochim. Acta* **64**, 1221–1228.

Fenter P., and Sturchio N. C. (1999) Structure and growth of stearate monolayers on calcite: First results of an in situ X-ray reflectivity study. *Geochim. Cosmochim. Acta* **63**(19/20), 3145–3152.

Fisler D. K., Gale J. D., and Cygan R. T. (2000) A shell model for the simulation of rhombohedral carbonate minerals and their point defects. *Am. Miner.* **85**, 217–224.

Geissbühler P., Fenter P., DiMasi E., Srajer G., Sorensen L. B., and Sturchio N. C. (2004) Three-dimensional structure of the calcite–water interface by surface X-ray scattering. *Surf. Sci.* **573**, 191–203.

Halgren T. A. (1992) Representation of van der Waals (vdW) interactions in molecular mecahnics force fields: Potential form, combination rules, and vdW parameters. *J. Am. Chem. Soc.* **114**(20), 7827–7843.

Hoover W. G. (1985) Canonical dynamics: equilibrium phase–space distributions. *Phys. Rev. A* **31**(3), 1695–1697.

Hwang S., Blanco M., and Goddard W. A. (2001) Atomistic simulations of corrosion inhibitors adsorbed on calcite surfaces I. Force field parameters for calcite. *J. Phys. Chem. B* **105**, 10746–10752.

Kerisit S., Marmier A., and Parker S. C. (2005) Ab initio surface phase diagram of the {1014} calcite surface. *J. Phys. Chem. B* **109**(39), 18211–18213.

Kerisit S., and Parker S. C. (2004a) Free energy of adsorption of water and calcium on the {10–14} calcite surface. *Chem. Commun.*, 52–53.

Kerisit S., and Parker S. C. (2004b) Free energy of adsorption of water and metal ions on the {10–14} calcite surface. *J. Amer. Chem. Soc.* **126**, 10152–10161.

Kerisit S., Parker S. C., and Harding J. H. (2003) Atomic simulation of the dissociative adsorption of water on calcite surfaces. *J. Phys. Chem. B* **107**, 7676–7682.

Kollman P. A. (1996) Advances and continuing challenges in achieving realistic and predictive simulations of the properties of organic and biological molecules. *Acc. Chem. Res.* **29**(10), 461–469.

Koneshan S., Rasaiah J. C., Lynden-Bell R. M., and Lee S. H. (1998) Solvent structure, dynamics, and ion mobility in aqueous solutions at 25 °C. *J. Phys. Chem. B* **102**, 4193–4204.

Krynicki K., Green C. D., and Sawyer D. W. (1978) Pressure and temperature dependence of self-diffusion in water. *Discuss. Faraday Soc.* **66**, 199–208.

Lamoureux G., and Roux B. (2003) Modeling induced polarization with classical Drude oscillators: theory and molecular dynamics simulation algorithm. *J. Chem. Phys.* **119**(6), 3025–3039.

Pavese A., Catti M., Price G., and Jackson R. (1992) Interatomic potentials for $CaCO_3$ polymorphs (calcite and aragonite), fitted to elastic and vibrational data. *Phys. Chem. Miner.* **19**, 80–87.

Pilson M. (1998) *An Introduction to the Chemistry of the Sea*. Prentice Hall, Englewood Cliffs, NJ.

Pokrovsky O. S., Mielczarski J., Barres O., and Schott J. (2000) Surface speciation models of calcite and dolomite/aqueous solution interfaces and their spectroscopic evaluation. *Langmuir* **16**, 2677–2688.

Pokrovsky O. S., and Schott J. (2002) Surface chemistry and dissolution kinetics of divalent metal carbonates. *Environ. Sci. Technol.* **36**, 426–432.

Pokrovsky O. S., Schott J., and Thomas F. (1999) Processes at the magnesium bearing carbonates/solution interface. I. A surface speciation model for magnesite. *Geochim. Cosmochim. Acta* **63**, 863–880.

Reeder R. J., Nugent M., Tait C., Morris D., Heald S., Beck K., Hess W., and Lazirotti A. (2001) Coprecitation of uranium(VI) with calcite: XAFS, micro-XAS, and luminescence characterization. *Geochim. Cosmochim. Acta* **65**, 3491–3503.

Rick S. W., and Stuart S. J. (2002) Potentials and algorithms for incorporating polarizability in computer simulations. *Rev. Comput. Chem.* **18**, 89–146.

Rohl A., Wright K., and Gale J. (2003) Evidence from surface phonons for the (2×1) reconstruction of the (10–14) surface of calcite from computer simulation. *Am. Miner.* **88**, 921–925.

Salinas-Nolasco M. F., Mendez-Vivar J., Lara V. H., and Bosch P. (2004) Passivation of the calcite surface with malonate ion. *J. Coll. Interfac. Sci.* **274**, 16–24.

Schlesinger W. H. (1997) *Biogeochemistry: An Analysis of Global Change*. Academic Press, New York.

Stahl G., Patzay G., Weiser L., and Kalman E. (2000) Study of calcite scaling and corrosion processes in geothermal systems. *Geothermics* **29**, 105–119.

Stumm W. (1992) *Chemistry of the Solid–Water Interface*. Wiley, London.

Stumm W., and Morgan J. J. (1996) *Aquatic Chemistry*. Wiley, London.

Teleman O., Jonsson B., and Engstrom S. (1987) A molecular dynamics simulation of a water model with intramolecular degrees of freedom. *Mol. Phys.* **60**, 193–203.

Teng H. H., Dove P. M., Orme C. A., and De Yoreo J. J. (1998) Thermodynamics of calcite growth: baseline for understanding biomineral formation. *Science* **282**, 724–727.

Titiloye J. O., de Leeuw N. H., and Parker S. C. (1998) Atomistic simulation of the differences between calcite and dolomite surfaces. *Geochim. Cosmochim. Acta* **62**, 2637–2641.

Titiloye J. O., Parker S. C., and Mann S. (1993) Atomistic simulation of calcite surfaces and the influence of growth additives on their morphology. *J. Cryst. Growth* **131**(3-4), 533–545.

Tosi M. P. (1964) Cohesion of ionic solids in the Born model. *Solid-State Phys.* **131**, 533–545.

van Cappellen P., Charlet L., Stumm W., and Wersin P. (1993) A surface complexation model of the carbonate mineral–aqueous solution interface. *Geochim. Cosmochim. Acta* **57**, 3505–3518.

van der Spoel D., van Maaren P. J., and Berendsen H. J. C. (1998) A systematic study of water models for molecular simulation: derivation of water models optimized for use with a reaction field. *J. Chem. Phys.* **108**(24), 10220–10230.

Verlet L. (1967) Computer 'experiments' on classical fluids. I. Thermodynamical properties of Lennard–Jones molecules. *Phys. Rev. A* **195**, 98–103.

Wang J., Kalinichev A. G., Kirkpatrick R. J., and Cygan R. T. (2005) Structure, energetics, and dynamics of water adsorbed on the muscovite (0 0 1) surface: a molecular dynamics simulation. *J. Phys. Chem. B* **109**, 15893–15905.

Wright K., Cygan R. T., and Slater B. (2001) Structure of the (10–14) surfaces of calcite, dolomite, and magnesite under wet and dry conditions. *Phys. Chem. Chem. Phys.* **3**, 839–844.

Associate editor: James Kubicki